Resident and Fellow Research Day 2025 – "Centennial Edition"

Department of Ophthalmology and Visual Sciences
University of Iowa Carver College of Medicine

Session I

Session II

Session III

Session IV

Session I – Paper 1

Cheryl Wang, MD | Rat Model of Type 2 Diabetes Mellitus Recapitulates Human Disease in the Anterior Segment of the Eye

Primary Supervisor: Mark Greiner, MD

Co-authors: Jessica M. Skeie, PhD; Chantal Allamargot, PhD; Andrew S. Goldstein, MD; Darryl Y. Nishimura, PhD; James M. Huffman, MD; Benjamin T. Aldrich, PhD; Gregory A. Schmidt, MBA, CEBT; Leandro B.C. Teixeira, DVM; Markus H. Kuehn, PhD; Mark Yorek, PhD

Purpose: Changes in the anterior segment due to type 2 diabetes mellitus (T2DM) are not well characterized, in part due to the lack of a reliable animal model. This study evaluates changes in the anterior segment, including crystalline lens health, corneal endothelial cell density, aqueous humor metabolites and ciliary body vasculature, in a rat model of type 2 diabetes mellitus (T2DM) compared with human eyes.

Methods: Sprague-Dawley male rats were fed a high fat diet (HFD, 45% fat) or normal diet, and HFD rats were injected intraperitoneally with streptozotocin (STZ) to create a model of T2DM. Microscopic analysis was performed to determine cataract formation and corneal endothelial cell density. Metabolomics of rat aqueous humor was performed to determine diabetes-related aqueous alterations. Transmission electron microscopy was used to assess qualitative ultrastructural changes of diabetic rat and human ciliary process microvessels at the site of aqueous formation.

Results: Diabetic rats demonstrated cataracts, lower corneal endothelial cell densities, altered aqueous metabolites, and ciliary body ultrastructural changes including vascular endothelial cell activation, pericyte degeneration, perivascular edema, and basement membrane reduplication. These findings recapitulated diabetic changes in human eyes.

Conclusions: Results support use of this model for studying ocular manifestations of T2DM and support a hypothesis postulating blood-aqueous barrier breakdown and vascular leakage at the ciliary body as a mechanism for diabetic anterior segment pathology.

Session I – Paper 2

Marshall Henrie, MD | A Novel Screening Method for Pediatric Keratoconus

Primary Supervisor: Kanwal Matharu, MD

Co-authors: Alina Dumitrescu, MD; Brian Young, BS, Grace Necker, BS

Purpose: This case-control retrospective study aims to develop a screening method for the early detection of keratoconus in children. Previous literature has described changes in corneal curvature, corneal thickness, and higher-order aberrations (HOAs) as a way of screening for disease and monitoring for progression of keratoconus in adults. Scheimpflug tomography (Pentacam) providers highly sensitive and specific tomographic indices for keratoconus diagnosis. Yet the equipment cost, examination time, and specialist interpretation required limit widespread screening, especially in primary-care or low-resource settings. Moreover, current consensus criteria omit HOAs, despite their routine capture during Pentacam studies. This research evaluates HOAs as a method of screening for keratoconus in children.

Methods: Data was obtained via chart review of patients age 7-17 seen at the University of Iowa from January 1st 2015 to January 1st 2025. Patients with a history of eye trauma, corneal crosslinking, corneal dystrophy, corneal scarring, exposure keratopathy or prior corneal surgery were excluded from this study. 14 eyes from 14 patients with a history of keratoconus and 14 eyes from patients without a history of keratoconus were included in this study. The average root-mean-squared (rms) of HOAs at both 6mm and 8mm optical zones were compared between the two groups with independent-samples t-tests.

Results: The mean rmsHOA for keratoconus patients at an 8mm optical zone = 5.96 compared to a mean = 1.32 for patients without keratoconus at 8mm ($p < 0.0004$). The mean at a 6mm optical zone for patients with keratoconus = 3.12 compared to a mean = 0.51 ($p < 0.0001$).

Conclusions: These results suggest HOAs may be a valid method for screening for keratoconus in pediatric patients. A larger data set is required to validate this method. A comparison of HOAs to astigmatism, central corneal thickness, and max Km will provide insight into how HOAs compare to current methods.

Session I – Paper 3

Brandon Baksh, MD and Jonathan Trejo, MD | The Effect of Intraoperative IOP Settings on the Rate of Post-CEIOL CME – Part 2

Primary Supervisor: Jaclyn M. Haugsdal, MD

Co-authors: David Chenoweth, BS; Mahsaw Mansoor MD; Matthew Meyer, MD; Thomas Oetting, MD

Purpose: Cystoid macular edema (CME) is a cause of decreased vision after cataract surgery (CS). Intraocular pressure (IOP) during CS may impact rate of CME. We analyzed the rate of CME after CS performed by two different surgeons using different IOP settings at University of Iowa.

Methods: Retrospective chart review of patients who underwent CS by a surgeon using high (O) or low (H) IOP settings from 6/1/2022 to 1/1/2024 at the University of Iowa. Rates of CME were analyzed. Patients with prior or active CME were excluded.

Results: 1335 patients had CS performed by O or H. 53 had post-operative CME. The rate of CME for H was 28/780 (3.59%) and O was 25/555 (4.5%), p-value 0.48.

Conclusion: CME rates were not different between two surgeons who use different IOP settings but otherwise operate similarly.

Session I – Paper 4

Zachary Richards, MD, MEngr | Identifying and Preventing Image Artifact in Microsurgical Video Captured with a Modular Stereo Camera

Primary Supervisor: Edward Linton, MD

Purpose: We have developed a stereo camera for operating microscopes based on a low-cost single board computer. Early tests contained significant compression artifacts, which detracted from video quality despite acceptable resolution and frame rate. This highlighted a need to improve video quality while working within the storage and hardware limitations of the device.

Methods: This study compared identical stereo videos of varying bitrate, which is inversely proportional to the degree of video compression. The Video Multimethod Assessment Fusion (VMAF) utility, a machine learning tool developed by Netflix and other researchers to predict subjective quality of a processed video, was used to compare these variably compressed videos to minimally compressed reference footage. The stereo camera itself consists of an inline two-port beamsplitter, cameras affixed to each port, and a Raspberry Pi-based single board computer which concatenates each camera's footage into a side-by-side video ready for viewing in a VR headset. A brief 1080p stereo video of a model eye with various microscope maneuvers was recorded for the purposes of this study at the maximal device bitrate of 10 megabits per second (Mbps). The reference video was compressed into 22 videos varying from 0.125 to 9.5 Mbps. Each video was compared to the reference with VMAF, yielding a quality score from 0 to 100 for each frame of video. The worst frame, best frame, and mean VMAF scores were recorded for each video, as well as the resulting file size of the compression process.

Results: File sizes ranged from 43.7 megabytes (10 Mbps bitrate, reference) to 0.6 megabytes (0.125 Mbps bitrate), with file size decreasing linearly with decreases in bitrate. Mean VMAF scores remained above 90 until bitrate dropped below 1.5 Mbps, while maintaining worst-frame VMAF scores above 90 required a bitrate above 3.5 Mbps. Best-frame scores, generally corresponding to frames with minimal motion, remained at 100 until compressed below 1 Mbps.

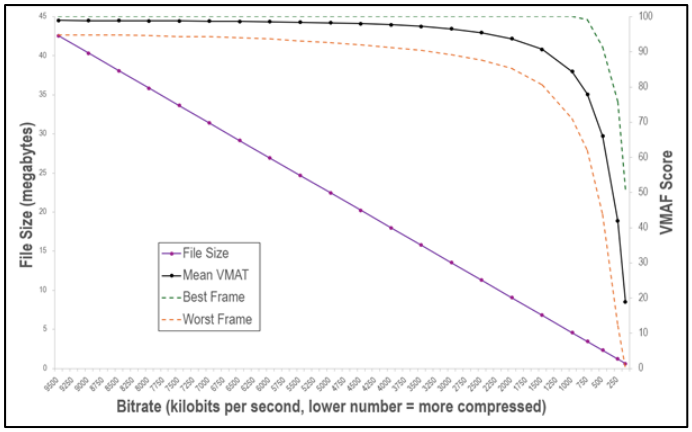

Conclusions: Artifacts are introduced with excessive compression, but significant reductions in file size are possible without sacrificing subjective quality. Balancing quality with file size is an essential task in storing lengthy surgical videos with sufficient quality for surgeon review and education.

Guadalupe Torres, MD | Comparison of "Corneal Cufflink" Plug Versus Standard of Care Plastic Disc Patch Gluing Methods to Seal Corneal Perforations: A Revision of Previous Protocols

Primary Supervisor: Christopher Sales, MD

Co-authors: Evan Balk, Luke Grandgenett

Purpose: Previously, a comparative study between cuff-link corneal plug and standard gluing methods resulted in the standard gluing method being ineffective in patching corneal holes, despite a history of demonstrated efficacy in clinical practice. The aim of this study was to replicate the success of corneal patching using standard methods in an ex vivo model in order to provide a reliable comparison for the efficacy of the corneal cufflink plug.

Methods: To address this issue the previous protocol for patching using a plastic disc was modified, including size of the plastic disc relative to the perforation and replication of anterior chamber with saline to allow for revision of leaks. Once a reliable protocol was established, the burst pressure for plugs and discs were directly compared using 2 and 3mm plugs versus 2 and 4mm discs to patch 1 and 2mm holes, respectively.

Results: The failure rate for the disc gluing method, burst pressure of 0mmg Hg, using our previous protocol was 4/10 compared to 0/10 using our new protocol. The average burst pressure using the prior disc gluing protocol was 51.4mm Hg (SD 67.16) compared to 289mm Hg (SD 90) using our current protocol. There was no significant difference in perforation size between patch and plug treatment groups for either the 1 mm ($P = 0.24$) or 2 mm diameter perforations ($P = 0.07$). In both groups, the plugs showed a trend toward greater strength than the patch in terms of burst pressure that did not reach statistical significance.

Conclusions: The success rate for corneal gluing in an ex vivo model using the plastic disc method increased with modification of the previous protocol. Decisions to increase the size of the plastic disc relative to the size of the perforation and to replicate an anterior chamber using saline were guided based on experience and more closely replicate corneal gluing outcomes in clinical practice. Our current protocol provides a more reliable comparison for the corneal cufflink plug. Future studies may focus on comparing the corneal cufflink plug and plastic disc gluing methods in rabbit eyes.

Session II – Paper 6

Joanna Silverman, MD | Effect of ocular trauma curriculum on preparing ophthalmology residents for surgical call

Primary Supervisors: Jaclyn Haugsdal, MD; Pavlina Kemp, MD

Purpose: Structured surgical curricula decrease intraoperative complications and enhance performance confidence. Operative management of open globes poses nuanced surgical demands and is infrequently simulated. The purpose of this study was to assess the efficacy of a new standardized surgical curriculum on preparing PGY4 ophthalmology residents to manage ocular trauma.

Methods: Eligible PGY4 residents attended a lecture and wet-lab simulation on open globe repair. Self-perceived preparedness via Likert scale (1-5) was determined prior, just after, and 10-weeks after educational intervention. PGY2-4 residents who attended lecture, but not wet-lab served as controls.

Results: Four PGY4 residents and 6 controls participated. Baseline confidence in open globe surgical management was statistically similar between groups (mean PGY4 3.17 [SD 1.86] vs control 1.0 [SD 0.0]; p=0.09), although skewed by one PGY4 with high pre-intervention confidence. Among PGY4s, confidence was unchanged immediately post-simulation (mean 3.03 {SD 1.44]; p=0.39) and increased, albeit insignificantly, at 10-weeks post-simulation (mean 4.4 [SD 0.56}; p=0.18). Longitudinal confidence remained significantly elevated amongst AGY4s compared to controls (mean 2.22 [SD 1.17]; p<0.005). Additionally, longitudinal confidence was elevated amongst PGY4s compared to controls regarding management of post-operative sequela (mean PGY4 4.75 [SD 0.55] vs control 3.5 [SD 1.26]; p=0.002).

Conclusions: This curriculum effectively increases self-perceived preparedness amongst residents managing ocular trauma, especially after practical call experience.

Session II – Paper 7

Bilal Ahmed, MD | *Design, Deployment, and Impact of the Iowa Ophthalmology Laser Curriculum*

Primary Supervisor: Jaclyn Haugsdal, MD

Co-author: Pavlina Kemp, MD

Purpose: To introduce and evaluate a structured, simulation-based curriculum designed to improve safety and efficacy in teaching ophthalmic laser procedures—specifically YAG capsulotomy and selective laser trabeculoplasty (SLT)—to beginning residents.

Methods: Ophthalmology residents participated in didactic and hands-on simulation sessions using SimulEye model eyes and departmental laser equipment under faculty supervision. A structured curriculum included lectures, procedural demonstration, and guided practice. Outcomes were measured using pre- and post-course knowledge assessments and self-reported confidence surveys.

Results: Residents showed statistically significant improvements in both procedural knowledge and confidence. Pre-course knowledge scores averaged 48% for YAG and 58% for SLT, increasing to 88% and 91% respectively post-course ($p < 0.05$). Confidence improved significantly in identifying indications, setting energy parameters, performing procedures, and managing post-treatment care. The increase in confidence was particularly notable for SLT, which is less commonly encountered in early training.

Conclusions: The Iowa Ophthalmology Laser Curriculum demonstrates that simulation-based training is an effective and safe method to teach laser procedures. Residents gained essential skills and confidence without patient risk. This novel approach addresses a previously underemphasized aspect of ophthalmology training and supports expanding simulation-based education to include laser techniques.

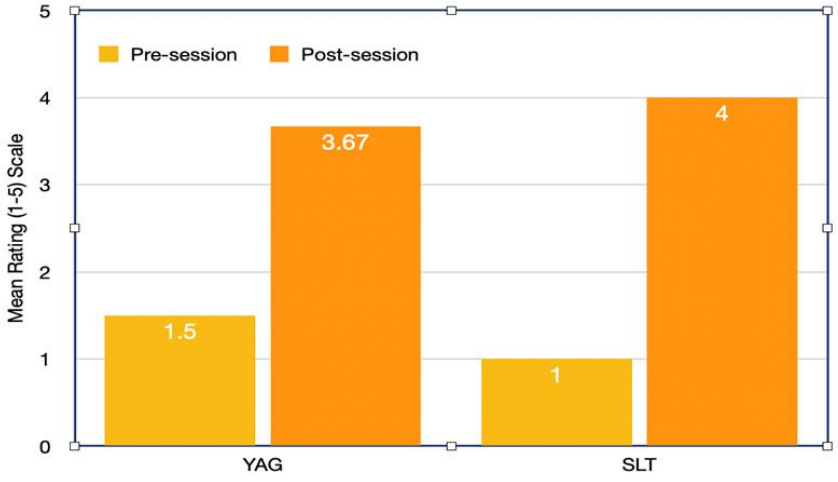

Session II – Paper 8

Oladipupo Anibire, MD and Donavon Dahmer, MD | Direct Selective Laser Trabeculoplasty versus Eye Drops for First-Line Treatment of Ocular Hypertension and Primary Open-Angle Glaucoma (DeLIGHT)

Primary Supervisor: Marc Toeteberg-Harms, MD

Purpose: Selective laser trabeculoplasty (SLT) and topical intraocular pressure (IOP)-lowering medications are both widely used as first-line therapies for ocular hypertension and primary open-angle glaucoma (POAG). This study will compare the anticipated efficacy and safety of direct SLT (DSLT) versus topical monotherapy as initial treatment in this patient population.

Methods: This retrospective cohort study will include patients from the University of Iowa Glaucoma Service who are newly diagnosed with ocular hypertension or mild to moderate POAG and initiated on either DSLT or a single topical IOP-lowering agent. The primary outcome will be the mean change in IOP over time. Secondary outcomes will include the incidence of post-DSLT IOP spikes and the need for additional therapy to manage the disease.

Results: We expect DSLT to be non-inferior to topical IOP-lowering medication. In addition, we expect DSLT to have a favorable safety profile and the incidence of post-laser IOP-spikes to be relatively rare.

Conclusions: This study aims to determine whether DSLT provides more effective and sustained IOP control compared to initial topical therapy in a US-based real-world setting. Findings may support evidence-based decision-making for first-line treatment of ocular hypertension and early POAG.

Andrew Zolot, MD | Postoperative Pilocarpine Use After Gonioscopy-Assisted Transluminal Trabeculotomy (GATT): A Retrospective Comparative Study of Intraocular Pressure Control and Medication Burden

Primary Supervisors: Erin Boese, MD; Andrew Pouw, MD

Co-authors: Joel VandeLune, BS; Quinton Christensen, BS; Aditya Somisetty, BS; Hansen Dang, BS

Purpose. Early IOP spikes are a recognized complication after GATT. Pilocarpine, a non-selective muscarinic agonist, contracts the ciliary muscle thereby expanding the trabecular meshwork and juxtacanalicular Schlemm's canal, theoretically enhancing aqueous outflow. We hypothesized that early post-operative pilocarpine use would reduce the incidence of spikes and improve long term IOP reduction.

Methods. A retrospective chart review was performed on 52 eyes (45 patients) that underwent GATT with or without phacoemulsification between 2017-2023. Post-operative pilocarpine (1 % q.i.d.) was used in 38 eyes; 14 eyes served as controls. An IOP spike was defined as either > 10 mmHg rise from baseline or any IOP > 30 mmHg within 28 days. Secondary endpoints were mean IOP change and glaucoma-drop burden (excluding pilocarpine) through 12 months.

Results. Pilocarpine and control cohorts were closely matched for age (60.7 ± 16.3 vs 61.1 ± 22.8 yr), baseline IOP (24.8 ± 9.5 vs 26.3 ± 7.9 mmHg), sex (70 % vs 57 % female) and rate of combined phaco-GATT (51 % vs 43). Early spikes occurred in 12/38 pilocarpine eyes (31.6 %) versus 1/14 control eyes (7.1 %), a difference that was not statistically significant. Across all eyes, mean IOP fell by 11.8 mmHg at 3 months and 10.8 mmHg at 12 months, with no inter-group difference at any visit. Mean glaucoma-drop burden declined from 3.25 ± 1.20 pre-operatively to 0.67 ± 1.11 at 12 months. Adding phacoemulsification to GATT did not measurably affect IOP lowering, regardless of pilocarpine use.

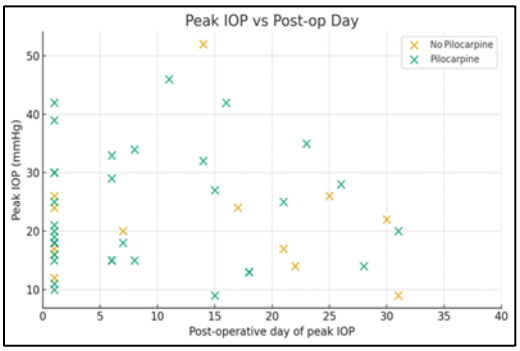

Conclusions. GATT ± phaco delivered a durable ≈ 11 mmHg IOP reduction and a three-drop decrease in medications at one year. Eyes treated with post-operative pilocarpine showed a higher but not statistically significant risk of early spikes. Possible explanations include miotic-induced blood aqueous barrier permeability, surgeon selection bias, detection bias from extra visits, and small event count. A larger prospective study is warranted to clarify whether pilocarpine materially alters spike risk and long term IOP.

Patrick Donegan, MD and Matthew Meyer, MD | Investigating the Safety and Efficacy of Baerveldt Drainage Implants with Modified Ventilating Sutures in Comparison to Non-Modified Baerveldt Drainage Implants and Ahmed Glaucoma Valves

Primary Supervisor: Andrew Pouw, MD

Co-authors: Kristin Davis, MS; Quinton Christensen, MS

Purpose: Baerveldt glaucoma implants (BGI) have proven efficacy in the management of glaucoma, however, these tubes take about 6 weeks to reach full effect. A ventilating suture modification to the traditional BGI (vsBGI) implantation technique allows for an earlier onset of IOP reduction. The safety and efficacy of the vsBGI has yet to be demonstrated. Here we compare IOP lowering efficacy of vsBGIs to Ahmed Glaucoma Valves (AGVs) at 1-year post-operation and compare the safety and efficacy of the vsBGI to unmodified BGI at the 3-months post-operation.

Methods: Patients ≥18 years with open-angle glaucoma who received a vsBGI, BGI, or AGV at the University of Iowa (2016-2024) were included in the study. Extracted data included IOP, visual acuity (VA), number and types of medications, and adverse events. Data was collected via manual chart review. A Chi-squared test was used to compare the number of patients exceeding target IOP at 1 year. A Mann-Whitney test was used to compare differences between groups at both pre-op and 3-month vs 1-year time points. P-values <0.05 were significant.

Results: Mean IOP change over 1 year was -13.5 mm Hg for vsBGI group vs -17.6 mm Hg for AGV group. IOP was significantly lower in the vsBGI group compared to BGI at 1 week (13.2 vs 18.2) ($p<0.0001$) but not at 3 months (15.7 vs 13.3) . There were 9.7% more instances of hyphema, 4.9% more corneal edema/graft worsening, 3.4% more CME, and 1.7% more surgical failures in the vsBGI group.

Conclusions: Initial data suggests no significant difference in medication number, visual acuity, or patients reaching target IOP between the vsBGI and AGV at 1 year. vsBGI is associated with a faster IOP reduction and fewer glaucoma medications at 3 months in comparison to BGI. There is potentially an increased risk of complications associated with the vsBGI compared to BGI.

Session III – Paper 11

Cy Lewis, MD, MPH | Using a Virtual Reality-Based 3D Atlas of the Eye for Training Medical Students to Evaluate Papilledema

Primary Supervisor: Edward Linton, MD

Co-authors: Brett Johnson, PhD, MS; Randy H. Kardon, MD, PhD; Michael Wall, MD

Purpose: Evaluating papilledema using direct ophthalmoscopy can be challenging for learners and non-ophthalmologists due to difficulty in mastering the examination technique and being able to recognize subtle three-dimensional (3D) optic disc features. This study aims to evaluate the effectiveness and student perception of a novel teaching modality employing a virtual reality (VR)-based atlas of the eye which uses using stereoscopic fundus photos to train medical students to recognize and grade papilledema.

Methods: During a six-month period, over 60 second- through fourth-year medical students (most not planning to specialize in ophthalmology) participated in a 2-week ophthalmology elective and received standardized training to evaluate papilledema. Objective assessment was conducted using pre- and post-testing to evaluate their ability to use Frisen grading (ground truth was determined with consensus by veteran neuro-ophthalmologists). Subjective feedback regarding ease of use, clinical utility, and perceived superiority over traditional methods was collected via a post-training survey.

Results: A statistically significant, albeit modest, improvement in papilledema evaluation was observed, with an increase in grading accuracy from 34% pre-training to 48% post-training after a single session ($p = 0.047$, $n = 19$). Participant perception of the VR training was overwhelmingly positive with 94% feeling more confident in recognizing papilledema, and 90% agreeing that stereoscopic fundus photos significantly improved their understanding of optic disc changes. Furthermore, 81% believed the skills gained would be helpful to them in future clinical practice. Regarding comparative benefits, 94% found the 3D VR atlas superior to standard 2D images for understanding papilledema, 97% agreed VR training offers unique advantages over traditional learning methods, and 90% believed it was easier to recognize papilledema signs in VR compared to direct or indirect ophthalmoscopy ($n = 31$).

Conclusions: A single training session with a 3D VR-based stereoscopic atlas significantly improved medical students' papilledema grading accuracy and was perceived very positively. Students found the tool enhanced their confidence and understanding, highlighted its utility for future practice, and considered it superior to traditional 2D learning and potentially easier than direct fundus observation for this specific task. We find this study has profound implications for improving medical education, particularly for non-ophthalmologists.

Session III – Paper 12

Jaffer Naqvi, MD | Distinguishing Papilledema from Pseudopapilledema with the Aid of Deep Learning Variational Autoencoders Trained on the Idiopathic Intracranial Hypertension Treatment Trial

Primary Supervisor: Edward Linton, MD

Co-authors: Cameron Keomanivong; Jui-Kai Wang, PhD; Randy Kardon MD, PhD

Purpose: To determine whether the spatial patterns encoded by a bi-channel deep-learning variational autoencoder (biVAE) model of retinal nerve fiber layer thickness and total retinal thickness from OCT in papilledema and normal subjects can improve OCT-based classification of papilledema vs pseudopapilledema.

Methods: A biVAE model was previously trained using 1498 optical coherence tomography (OCT) scans of 125 subjects over time from the Idiopathic Intracranial Hypertension Treatment Trial (IIHTT). An independent test data set of 371 eyes from 193 papilledema subjects and 21 eyes from pseudopapilledema subjects from our institution was collected, and the two latent variables (i.e., d1 and d2; low-dimensional representation) that the biVAE used to reconstruct the retinal nerve fiber layer (RNFL) thickness maps were collected from the model, as they contain information about the spatial pattern of the RNFL thickness map. We generated three binary logistic regression models to distinguish papilledema from pseudopapilledema based on the following parameters: 1) the peripapillary RNFL thickness (pRNFLT), 2) the latent variables d1 and d2 from the biVAE model and 3) the latent variables from the biVAE plus the optic nerve head volume. Models were trained with a 2:1 papilledema:pseudopapilledema ratio of training images using leave-one-subject-out cross-validation. Area under the receiver operating characteristic curves for classification from each group were compared.

Results: Receiver operating characteristic (ROC) curves for each of the three classification models and their area under curves (AUCs) were generated. Model 1 incorporated only the pRNFLT and produced an AUC of 0.45. Model 2 incorporated only spatial information contained within latent variables d1 and d2 and produced an AUC of 0.71. Model 3 included both spatial information contained within the latent variables and the ONHV and produced the highest AUC of 0.75.

Conclusion: The spatial information encoded by the biVAE latent variables are able to perform modest discrimination of papilledema from pseudopapilledema, indicating that the RNFL patterns represented by the model preserve their clinical meaning.

Session III – Paper 13

Adetayo Oladele-Ajose, MD | Improving Utilization of Artificial Intelligence based Diabetic Retinopathy Screening by Addressing Patient and Provider Concerns

Primary Supervisor: Kanwal Matharu, MD

Co-authors: Taariq Mohammed, MD; Khadija Shahid, OD, MPH, FAAO; David Chenoweth BS; Vera Howe OD, FAAO; Kylee Bradley, BSN, MSN; Elliott Sohn MD, FASRS, FARVO

Purpose: Diabetic retinopathy (DR) is the primary cause of preventable blindness in America and a growing issue internationally. Screenings are essential to patient health and required by Medicare reimbursement guidelines. The satellite clinic of a tertiary care referral center has had an FDA-Approved IDx-DR autonomous diagnosis of DR for three years but with low utilization. Our group sought to understand patient and provider attitudes towards IDx screenings, then improve utilization.

Methods: A 4-question survey was emailed to primary care providers to measure their perspectives towards IDx. Patients were offered a 3-question survey after screening. Responses were sorted by a single reader into 4 categories. Provider feedback guided educational interventions regarding IDx. Starting in April 2024, eye care and primary care providers met monthly to discuss IDx. The primary outcome was number of IDx referrals 10 months before and after the intervention. An unpaired t-test with unequal variance was used to analyze statistical significance. Secondary outcomes included qualitative feedback from patients and providers regarding their experience using IDx.

Results: Of 23 providers who were surveyed, 22 replied. 95% of survey participants reported that they were aware of IDx, but only 73% of respondents reported comfortability with IDx technology. From July 2023 to April 2024, there were 37 referrals total for IDx screening. After the intervention point, from May 2024 to February 2025, there were 137 screening referrals ($p < 0.00186499$) (Figure 1). 36 patients completed post-screening surveys. 86% of surveyed patients preferred IDx screening to scheduling for annual dilated eye exam. 86% of surveyed patients planned to repeat IDx screening next year. 61% of patients felt like they would still like to see an eye doctor in addition to IDx screening, whereas 38% of patients felt either neutral or like they did not need to see an eye doctor in addition to screening.

Summary of barriers to utilization of screening tool

Concern	Perception	Education
Cost	"I'm not entirely sure if this is covered by patients' insurances or not."	In August 2020, the Centers for Medicare and Medicaid Services (CMS) announced coverage of CPT code 9225X for autonomous AI.
Availability and Awareness	"I wasn't aware of this until recently." "I was unaware that it was available again."	IDx is available for screening at our satellite clinic.
Workflow	"It's unclear how easy it is to schedule." "Patient's aren't sure if they can get same day appointments."	IDx screening takes 5-10 minutes and can be done as an undilated exam, on the same day as long as there is an available trained technician.
Efficacy	"Is this an adequate substitute for a comprehensive eye exam?" "Patient's may not trust the technology since they do not see a doctor." "Patient's often have other eye concerns."	IDx serves as a screening tool. If patient's have additional eye-related concerns, they are able to schedule with an optometrist or ophthalmologist right after undergoing IDx screening. A 2020 validation study of 2680 subjects compared IDx grading of diabetic retinopathy with manual grading by ophthalmologists. This study demonstrated IDx's ability to diagnose diabetic retinopathy and macular edema in patients with diabetes with 100% sensitivity and 82% specificity. IDx was also the first autonomous artificial intelligence system to be FDA-Approved across the field of medicine and has been integrated into the American Diabetes Association's "Standard of Diabetes Care"

Conclusions: By meeting with healthcare providers regularly to discuss concerns and obstacles regarding IDx, there was a significant increase in its utilization. Patients reported a strong preference towards AI based screening as well. These results suggest that successful implementation of IDx screening requires regular, tailored education of providers for maximum impact.

Matthew Hunt, MD | Commercial, Off-the-Shelf Multimodal AI Models for Autonomous AI Diabetic Eye Exams

Primary Supervisor: Michael D. Abràmoff, MD, PhD

Co-authors: Tinglong Dai, PhD

Purpose: Autonomous AI for diabetic eye exams is among the most validated and trusted medical AI systems, yet adoption remains limited. In contrast, commercially available off-the-shelf generative AI models (OTSAIs) are being rapidly tested in medical settings despite a lack of such real-world validation. These models have shown strong performance on medical reasoning tasks, prompting interest in their potential for clinical deployment. In this study, we evaluate the ability of four OTSAIs to detect more-than-mild diabetic retinopathy from fundus photos and assess their performance in relation to regulatory requirements for autonomous diagnostic devices.

Methods: We evaluated four OTSAIs —GPT-4o and GPT-4o-mini, Grok, and Gemini against the Messidor-2 dataset (over 1700 fundus photos) with a level 3 reference standard using three prompting strategies. All models were accessed via the application programming interfaces (APIs), with over 47,000 images in total fed into the models. ROC analysis was conducted at the subject level.

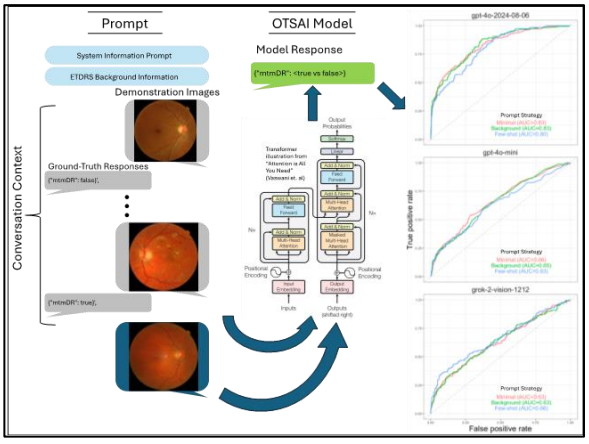

Figure: Data processing pipeline – few-shot prompting with multiple examples giving context for the OTSAI model. ROC curves generated for each model and prompting strategy with AUCs are shown

Results: The best-performing OTSAI, GPT-4o—despite not being explicitly trained for any medical imaging task—achieved an AUC of 0.86, and a sensitivity of 88% at a specificity of 63%, determined at the threshold where the lower bound of the 95% confidence interval for sensitivity exceeded 80%. It does not meet human performance, with expert retina specialists demonstrating an AUC of 0.94 against that same reference standard, nor does it meet workflow requirements – the images in Messidor-2 were obtained by expert photographers. False-negative predictions most often occurred in less-severe cases—such as those with single retinal hemorrhages—which are also challenging for human experts.

Conclusions: Emergent (i.e. for which they were not trained) OTSAI performance does not meet regulatory thresholds for autonomous AI devices. However, OTSAI performance on medical reasoning tasks, combined with this emergent performance on a specific diagnostic task, allows perspective on a regulatory alternative to the FDA medical-device clearance pathway. A task-specific licensing – resembling physician-assistant licensure by State Medical Boards – could allow bundled OTSAIs to improve patient outcomes by expanding access quickly. This may, however, limit outcome improvement compared to the quality and cost improvements achieved with the superhuman accuracy of true medical-device autonomous AI.

Session III – Paper 15

Richard Yi, MD | Immune Dysfunction in Diabetic Macular Edema: Uncovering Pathways for Enhanced Treatment

Primary Supervisor: Elliott Sohn

Co-authors: Srinivas Chava, Christine Sinkey, Farhad Salari, Zeb Zacharias, Jon Houtman

Purpose: To explore the role of T-cell dysfunction in patients with nonproliferative diabetic retinopathy with diabetic macular edema. Our focus is on how different groups respond variably to different treatment types (i.e. intravitreal anti-VEGF versus steroid). We hypothesize that the subset of patients whom are minimally responsive to standard intravitreal anti-VEGF treatments will have findings suggestive a proinflammatory state.

Methods: We will start out by recruitment of patients under different treatment groups (anti-VEGF and steroid) and control (nonproliferative diabetic retinopathy without diabetic macular edema). Inclusion – patients older than 18 years of age with nonproliferative diabetic retinopathy and diabetic macular edema. Exclusion – patient with recent infectious illnesses, malignancy, active autoimmune or connective tissue disorder, use of immunosuppressive agents, or other ocular conditions commonly known contribute to macular edema (e.g. retinal vein occlusion). After obtaining the patient's consent, we will proceed with collecting blood sample in all three groups along with aqueous samples in the treatment groups. Samples will be analyzed in the lab using established methods (23-color, 29-color and 31-color spectral flow cytometry panels) to characterize T-cells and antigen presenting cells along with other inflammatory markers.

Results: Collection is in progress with samples from 8 patients who meet the criteria collected. Analysis will take place once the sample collection is completed.

Conclusions: We hope to better understand the effects of pro-inflammatory factors on patients with nonproliferative diabetic retinopathy with diabetic macular edema, especially those resistant to anti-VEGF treatments. With more insight, we will be able to further tailor the treatments for our patients and identify potential therapeutic targets in the future.

Arnulfo Garza Reyes, MD | Pigmentation Artifact of Broad Wavelength Light Emitting Diode Illumination "True-color" Fundus Photography in Circumscribed Choroidal Hemangiomas

Primary Supervisor: Elaine Binkley, MD

Co-authors: Farzad Jamshidi, MD, PhD; Connie Hinz, COT; H. Culver Boldt, MD

Purpose: Color characterization plays an important role in the diagnosis of choroidal hemangiomas. Hence, fundus photography is a critical ancillary test in the recognition of this disease. We report a color artifact with "true-color" fundus imaging that can lead to a more pigmented appearance of these lesions resulting in incorrect diagnosis.

Methods: This was a single center retrospective study with chart and imaging review of patients with a diagnosis of choroidal hemangioma from October 2007 to October 2024. Fifteen cases with multimodal confirmation of the diagnosis with fundus photography, indocyanine green (ICG) angiography, standardized echography, and optical coherence tomography (OCT) were identified. All cases had fundus imaging with at least 2 different cameras. Pigmentation was graded by a retina specialist and the different fundus photography modalities as well as fundus examinations were compared.

Results: 9 cases had artifactual "true-color" fundus photography with pigmentation. 6 cases had a referring diagnosis of choroidal nevus or melanoma. All cases had multimodal imaging with a diagnosis confirming the diagnosis of choroidal hemangioma. 10 of 15 patients received photodynamic therapy (PDT) while 5 were observed. The average follow-up for patients was 36 months.

Conclusion: Pigmentation artifact can be present in fundus photography of choroidal hemangiomas even with "true-color" fundus cameras. The Xenon lamp-based cameras tend to produce the most clinically accurate photos. This paper highlights the critical value of the clinical exam for the evaluation of choroidal hemangiomas.

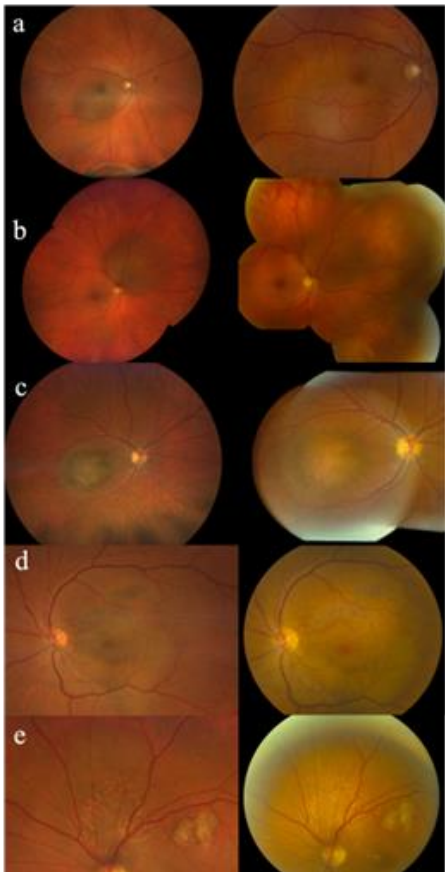

Figure. Clarus versus Topcon fundus images of choroidal hemangiomas. Images on the left of each pair show choroidal hemangiomas captured by Clarus 500 cameras, Topcon fundus photos are shown on the right. There appears to be a brown pigmented appearance to the Clarus 500 "true-color" images that could lead to an incorrect diagnosis of melanocytic lesions.

Kyle Green MD | Post-operative intraretinal hemorrhages following retinal detachment repair

Primary Supervisor: Jonathan Russell, MD, PhD

Purpose: To present a case series of patients that developed intraretinal hemorrhages following retinal detachment repair. The mechanism of this finding is unclear.

Methods: Cases demonstrating this phenomenon were obtained from multiple surgeons at the University of Iowa. A chart review was performed to compare characteristics of the patients, the surgeries performed, and the distribution and duration of the hemorrhages.

Results: 7 eyes in 7 patients were found to have intraretinal hemorrhages in their post-operative course following retinal detachment repair. The hemorrhages were variable in their size and distribution. All 7 eyes underwent pars plana vitrectomy and 5 of the eyes had a scleral buckle placed either at the time of surgery or during a prior surgery. At the time of surgery, 5 eyes had silicone oil inserted, and 2 eyes were filled with gas. 1 patient had a history of ocular hypertension related to trauma, and 1 had a history of mild non-proliferative diabetic retinopathy.

Conclusions: While the mechanism is unclear, we hypothesize the intraretinal hemorrhages following retinal detachment repair in these cases may relate to intraocular pressure changes akin to decompression retinopathy.

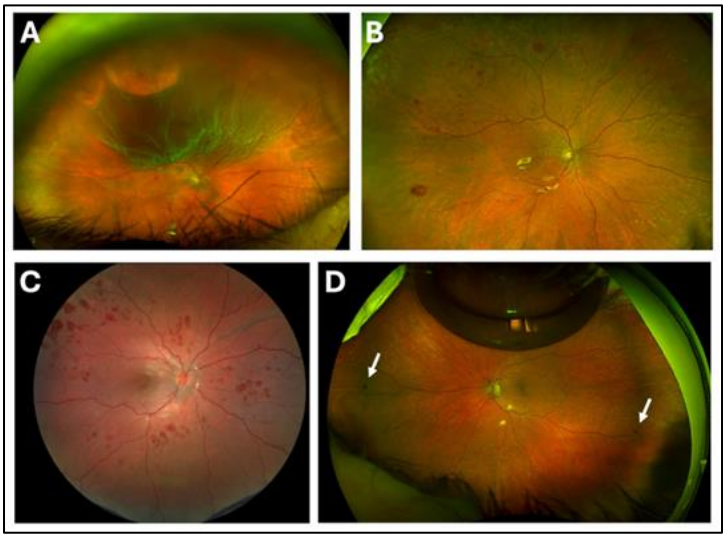

Figure: Examples of post-operative intraretinal hemorrhages. (A-B) Pre- and post-operative photos of a patient with a macula-involving retinal detachment who developed intraretinal hemorrhages seen 9 days following repair with vitrectomy and silicone oil. (C) Post-operative photo of a patient who similarly developed intraretinal hemorrhages seen 5 days following repair with vitrectomy and silicone oil (D) Post-operative photo of a patient who developed intraretinal hemorrhages (arrows) seen 6 weeks following repair with vitrectomy and C3F8 gas (earlier post-operative photos limited by gas bubble).

Taariq K. Mohammed, MD | Cystoid Macular Edema in Retinitis Pigmentosa: Evidence toward a Theory of Impaired Fluid Clearance

Primary Supervisor: Ian C. Han, MD

Co-authors: Kyle M. Green, MD; D. Brice Critser, BS, CRA; Edwin M. Stone, MD, PhD

Purpose: The pathophysiology of cystoid macular edema (CME) in retinitis pigmentosa (RP) remains unclear. We hypothesize that accumulation of intraretinal fluid may result from impaired clearance, in contrast to vascular leakage which is present in other conditions like diabetic macular edema. The purpose of this study was to use swept source optical coherence tomography angiography (SS-OCTA) to elucidate the spatial relationship of CME in RP with the deep capillary plexus (DCP) and external limiting membrane (ELM), key anatomic structures in retinal fluid clearance.

Methods: This was a retrospective cross sectional study following consecutive patients with molecularly confirmed RP associated with *USH2A*, *RHO*, or *RPGR*. In all patients, a comprehensive ophthalmic examination was performed including SS-OCTA (Zeiss Plex Elite 9000) of the macula. The OCTA images were segmented and analyzed in a semi-automated fashion to identify the spatial overlap of areas of CME, DCP loss, and EZ and ELM preservation (Figure 1).

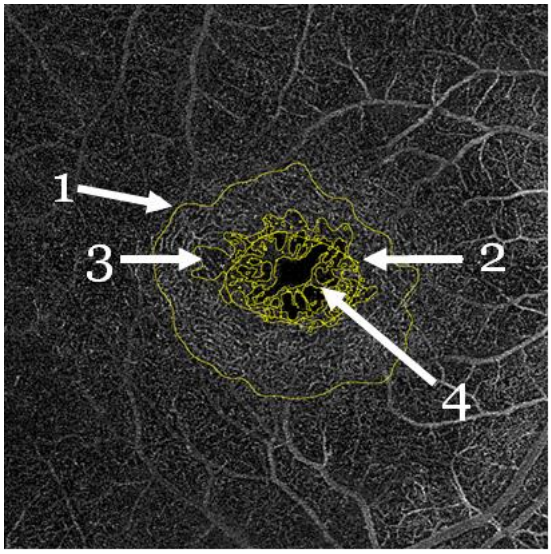

Figure. Example of SSOCTA segmentation showing relative overlap of areas of ELM preservation (1), EZ preservation (2), DCP loss (3), and CME (4).

Results: 129 eyes of 70 patients with RP were included (29 eyes associated with *RHO*, 39 eyes with *RPGR*, and 61 eyes with *USH2A*). The mean age was 37 (range 6-78), the mean best corrected visual acuity was 0.35 logMAR, and the prevalence of CME was 31% (10% in *RPGR*, 26% in *USH2A*, 48% in *RHO* ($p = 0.002$)). In patients with CME, areas of CME had 97% spatial overlap with areas of ELM preservation, 66% spatial overlap with areas of EZ preservation, and 83% spatial overlap with areas of DCP loss.

Conclusions: The prevalence of CME varies by genotype. In all patients with CME, the areas of intraretinal fluid had a strong tendency to occur in areas of ELM preservation and DCP loss, and a moderate tendency to occur in areas of EZ preservation. Abnormal fluid clearance mediated by Muller cells though the DCP and ELM may play a role in the development of CME in RP.

Nicole Somani, MD, MPH | Nonsyndromic Autosomal Recessive Retinitis Pigmentosa Caused by Mutations in the TMEM216 Gene

Primary Supervisor: Edwin Stone, MD, PhD

Purpose: To characterize the clinical phenotype associated with *TMEM216* mutations in a cohort of patients, primarily of African ancestry, and to assess the natural history and retinal findings associated with this genotype.

Methods: Retrospective chart review of eight patients with *TMEM216*-associated retinal degeneration. Demographic, visual acuity, refractive, structural, and longitudinal follow-up data were extracted from medical records. Presence of systemic ciliopathy features was also assessed.

Results: Seven of the eight patients were confirmed to be of African ancestry, and all seven were homozygous for a guanine-to-thymine substitution in *TMEM216*, 69 bases upstream of the start codon. In our cohort of patients, this variant accounts for approximately 10% of retinitis pigmentosa among African Americans. The one non-African American patient was a compound heterozygote for *TMEM216*, harboring a CGA>TGA nucleotide substitution resulting in an amino acid change of Arg85Stop and a novel C>T nucleotide substitution 71bp upstream of the start codon. The age of onset of the eight patients ranged from 3 to 19 years, with nyctalopia as the universal presenting symptom. At presentation, 7 of 8 patients had visual acuity of 20/50 or better in at least one eye. Three patients met criteria suggestive of Leber Congenital Amaurosis (LCA) spectrum disorders based on early-onset presentation. Refractive error ranged from -6.50 to -0.625 diopters (mean ± SD: -4.56 ± 1.82). Retinal findings consistent with retinitis pigmentosa were present in all patients, including midperipheral pigmentary changes, vessel attenuation, and waxy disc pallor. Macular pigmentary mottling was observed in three patients ≥34 years of age. Cystoid macular edema was present in 9 of 16 eyes. No patients demonstrated systemic features of ciliopathy. Longitudinal data were available for two patients, with the longest follow-up spanning 40 years. By the fifth decade of life, 2 of 3 patients with available data had visual acuity of 20/125 or worse in both eyes.

Conclusions: *TMEM216*-associated retinopathy is characterized by early nyctalopia, midperipheral retinal degeneration, and relative central visual acuity preservation into mid-life. These findings underscore the importance of recognizing *TMEM216* as a cause of autosomal recessive retinal dystrophy, particularly in individuals of African ancestry.

Paper 20

Rupin Parikh, MD | Blinded by the Flames: Evaluation of Novel Guidelines for Management of Burn Patients at Risk of Orbital Compartment Syndrome

Primary Supervisors: Chau Pham MD, FACS; Keith Carter MD, FACS; Erin Shriver MD, FACS

Co-Authors: Julia Fleecs BS; Jamie Keen MD; Grace Lee MD; Samuel Jones MD FACS

Purpose: Orbital compartment syndrome (OCS) is a devastating complication in burn patients that can lead to permanent vision loss and blindness. The Burn Orbital Compartment Syndrome guidelines (BOCS) were developed and initiated in 2020 to incorporate the previously reported significant OCS risk factors (>50% total body surface area (TBSA) involving the face) and likely risk factors identified at the study institution (vasopressor use, albumin use, and the presence of conjunctival chemosis) into a framework to direct initiation and frequency of intraocular pressure (IOP) measurements and timing of surgical intervention. The aim of this study is to evaluate the use of BOCS in detecting IOP elevation and preventing vision-threatening OCS in burn patients.

Methods: A 4-year retrospective review was performed to evaluate burn patients with facial involvement managed by ophthalmology using BOCS. Patients were divided into *High Risk* versus *Low Risk* and *Surgical* versus *Non-surgical* groups. *High Risk* patients had > 50% TBSA involving the face or at least 2 of 3 likely risk factors (vasopressin use, albumin use, or presence of conjunctival chemosis) with exams every 4 hours. Other patients (*Low Risk)* were checked every 8 hours. The *Surgical* group underwent interventions including canthotomy and cantholysis, septolysis, and/or eyelid split.

Results: Vasopressor administration was found to be significantly more frequent only in *High Risk* patients (92.3%) compared to *Low Risk* patients (18.2%, $p<0.05$). Presence of conjunctival chemosis was not significantly different in either comparison group. Surgical intervention was performed on 61.5% of *High Risk* patients, while 88.9% of *Surgical* patients were *High Risk*. *Surgical* patients had higher mean %TBSA (61.0%) and albumin administration rates (88.9%) compared to the *Non-surgical* group (22.3% TBSA, 20% albumin use; $p<0.05$). Mean peak IOP in the *Surgical* group was 28.4 mmHg (range 11-80) and occurred at 11.8 hours post-injury (range 5-20).

Conclusions: Early and frequent IOP monitoring is essential in *High Risk* burn patients. Eye examinations should occur within 12 hours with adjustments in frequency based on risk factors like %TBSA and albumin use. Broader implementation and analysis of BOCS, combined with collaboration with burn centers nationally and internationally, will help refine OCS management strategies and enhance prevention efforts, ultimately reducing the risk of this devastating complication.

Table 2. Patient demographics and clinical characteristics

	Total (n=24)	**Surgical** (n=9)	**Non-surgical** (n=15)	**p-value**	**High Risk** (n=13)	**Low Risk** (n=11)	**p-value**
Age ± SD (yr)	41.5 ± 23.1	39.6 ± 19.0	43.7 ± 23.1	0.693	42.4 ± 19.7	41.8 ± 24.0	0.8087
Male (%)	14 (58.3%)	8 (88.9%)	6 (40.0%)	**0.0333**	10 (76.9%)	4 (36.4%)	0.0953
Mortality (%)	4 (16.7%)	2 (22.2%)	2 (13.3%)	0.6146	4 (30.8%)	0 (0%)	0.0983
% TBSA burned ± SD	36.8% ± 30.7%	61.0% ± 23.8%	22.3% ± 25.0%	**0.0014**	59.2% ± 23.8%	10.4% ± 8.53%	**<0.0001**
Albumin administered (%)	11 (45.8%)	8 (88.9%)	3 (20.0%)	**0.0022**	11 (84.6%)	0 (0%)	**<0.0001**
Vasopressor administered (%)	14 (58.3%)	7 (77.8%)	7 (46.7%)	0.2099	12 (92.3%)	2 (18.2%)	**0.0005**
Conjunctival chemosis (%)	18 (75.0%)	9 (100%)	9 (60.0%)	0.0519	12 (92.3%)	6 (54.5%)	0.0608
High Risk patients (%)	13 (54.2%)	8 (88.9%)	5 (33.3%)	**0.0131**	---	---	---
Surgical patients (%)	9 (37.5%)	---	---	---	8 (61.5%)	1 (9.09%)	**0.0131**
Mean initial IOP (mmHg)	22.7	28.4	19.2	**0.0362**	26.8	17.9	**0.0011**
Mean peak IOP (mmHg)	31.9	47.8	22.3	**<0.0001**	41.5	21.9	**<0.0001**
Initial IOP <30 mmHg	19 (79.2%)	5 (55.6%)	14 (93.3%)	**0.0474**	9 (69.2%)	10 (90.9%)	0.3271
Peak IOP >35 mmHg	8 (33.3%)	8 (88.9%)	0 (0.0%)	**<0.0001**	8 (61.5%)	0 (0%)	**0.002**
Brimonidine started at onset (%)	10 (41.7%)	7 (77.8%)	3 (20.0%)	**0.0104**	9 (69.2%)	1 (9.09%)	**0.0045**
Mean final visual acuity (LogMAR)	0.0842	0.157	0.0374	**0.0239**	0.131	0.0374	0.0642

% TBSA, Percentage of total surface body area burned (all patients with facial involvement); SD, standard deviation; OCS, orbital compartment syndrome; IOP, intraocular pressure
High Risk patients include patients with at least >50% TBSA involving the face, or two of the three risk factors of albumin use, vasopressor use, or conjunctival chemosis
Surgical patients include patients that underwent interventions including canthotomy and cantholysis, septolysis, and/or eyelid split
Risk factors highlighted in gray
Bolded p-values indicate statistical significance (<0.05)